The EMBO Journal Vol. 22 No. 14 pp. 3602–3612, 2003

WAVE2 deficiency reveals distinct roles in embryogenesis and Rac-mediated actin-based motility

Catherine Yan[1,2,3], Narcisa Martinez-Quiles[4,5], Sharon Eden[6], Tomoyuki Shibata[7,8], Fuminao Takeshima[7,8], Reiko Shinkura[9], Yuko Fujiwara[9,10], Roderick Bronson[11], Scott B.Snapper[7,8], Marc W.Kirschner[6], Raif Geha[4,5], Fred S.Rosen[1,2,5] and Frederick W.Alt[1,2,3,5,9,12]

[1]Center for Blood Research, 200 Longwood Avenue, Boston, MA 02115, [2]Department of Medicine, [4]Division of Immunology, [9]Howard Hughes Medical Institute, [10]Division of Hematology and Oncology, Children's Hospital, Boston, MA 02115, Departments of [3]Genetics, [5]Pediatrics, [6]Cell Biology, [7]Medicine and [11]Pathology, Harvard Medical School, Boston, MA 02115 and [8]Gastrointestinal Unit (Medical Services) and the Center for the Study of Inflammatory Bowel Disease, Massachusetts General Hospital, 55 Fruit Street, Boston, MA 02115, USA

[12]Corresponding author
e-mail: alt@enders.tch.harvard.edu

The Wiskott–Aldrich syndrome related protein WAVE2 is implicated in the regulation of actin-cytoskeletal reorganization downstream of the small Rho GTPase, Rac. We inactivated the WAVE2 gene by gene-targeted mutation to examine its role in murine development and in actin assembly. WAVE2-deficient embryos survived until approximately embryonic day 12.5 and displayed growth retardation and certain morphological defects, including malformations of the ventricles in the developing brain. WAVE2-deficient embryonic stem cells displayed normal proliferation, whereas WAVE2-deficient embryonic fibroblasts exhibited severe growth defects, as well as defective cell motility in response to PDGF, lamellipodium formation and Rac-mediated actin polymerization. These results imply a non-redundant role for WAVE2 in murine embryogenesis and a critical role for WAVE2 in actin-based processes downstream of Rac that are essential for cell movement.

Keywords: actin polymerization/lamellipodium/Rho GTPase/WASP-related protein/WAVE

Introduction

Actin polymerization is required for diverse cellular processes, including cell growth, motility and polarization. The transduction of extracellular stimuli to reorganize cortical actin filaments is governed by small Rho GTPases, Cdc42 and Rac, which stimulate polarized forward protrusions (filopodia and lamellipodia) at the leading edge of cells, and RhoA, which induces retractions at the tail end of cells. The Wiskott–Aldrich syndrome protein (WASP) family, referred to as WASPs (WASP and N-WASP) and SCAR/WAVEs (WAVE1, WAVE2 and WAVE3), are cytoplasmic molecules that link Rho GTPases and actin assembly (Suetsugu *et al*., 1999; Takenawa and Miki, 2001). In response to activation of small Rho GTPases, these proteins stimulate the nucleating activity of the Arp2/3 complex, resulting in specific cell surface projections: filopodia by N-WASP following activation by Cdc42, and lamellipodia by WAVE molecules following activation by Rac (Miki *et al*., 1998a,b; Takenawa and Miki, 2001).

One SCAR/WAVE protein exists in *Dictyostelium discoideum*, *Caenorhabditis elegans* and *Drosophila melanogaster*, and three orthologs (WAVE1, WAVE2 and WAVE3) are conserved in mammals (Bear *et al*., 1998; Suetsugu *et al*., 1999; Benachenhou *et al*., 2002). WAVE1 and WAVE3 are predominantly expressed in the brain; like N-WASP, WAVE2 is widely expressed (Bear *et al*., 1998; Suetsugu *et al*., 1999; Benachenhou *et al*., 2002; Soderling *et al*., 2003). SCAR/WAVE proteins were first identified in *Dictyostelium* as negative regulators of G protein coupled signaling (Bear *et al*., 1998) and in transient assays as a downstream effector for Rac-mediated lamellipodia formation (Miki *et al*., 1998b). In *Dictyostelium*, *scar*-deficient cells generated by homologous recombination display aberrant morphology and actin distribution during chemotaxis, reduced F-actin staining during vegetative growth, and reduced fluid phase influx and endocytic trafficking (Bear *et al*., 1998; Seastone *et al*., 2001). In *Drosophila*, inactivation of the single *SCAR/WAVE* gene shows the encoded protein plays the major role in Arp2/3-dependent regulation of cell morphology, whereas WASP appears to be largely dispensable (Zallen *et al*., 2002). The conserved Verprolin-cofilin-acidic (VCA)-rich domain in both WASPs and WAVEs mediates binding and activation of Arp2/3 catalysis of actin polymerization (Machesky and Insall, 1998; Miki *et al*., 1998b; Suetsugu *et al*., 1999; Zalevsky *et al*., 2001). In contrast to WASPs, WAVEs share a common SCAR homology domain and are missing the Cdc42/Rac interactive binding (CRIB) domain that mediates WASPs interaction and activation by Rho GTPases (Suetsugu *et al*., 1999; Kim *et al*., 2000).

The mechanism of regulation and activation of WASPs and WAVEs are different. In the case of WASPs, the VCA domain is autoinhibited by intramolecular interactions with the CRIB domain (Kim *et al*., 2000) and activated by interactions with GTP–Cdc42 and phosphatidylinositol-4,5-biphosphate. In contrast, the full-length recombinant WAVE1 protein is constitutively active (Machesky *et al*., 1999), whereas *in vivo* it is maintained in an inactive heteropentameric complex that includes WAVE, the p53-inducible PIR121, the Nck-associated protein Nap125, the Abl interactor protein Abi2 and a small actin-stimulating

peptide, HSPC300 (Eden *et al*., 2002). Activated Rac or the Src homology 3 (SH3)–SH2 adaptor protein Nck dissociates the WAVE complex to release the active WAVE–HSPC300 complex to promote actin nucleation (Cory and Ridley, 2002; Eden *et al*., 2002). Rac signaling to actin is then proposed to be attenuated by recruitment of the Rac-selective GTPase activating protein WRP by WAVE1, which hydrolyzes Rac to the inactive GDP bound form (Soderling *et al*., 2002). Currently, the rapidly expanding list of WAVE protein partners includes cytoskeletal components (profilin, α-tubulin and spectrin αII and βIII) and SH3 proteins involved in signal transduction linked to WASPs and Rho GTPase, Ras and Rab GTPase pathways (Miki *et al*., 1998b, 1999, 2000; Pollard *et al*., 2000; Westphal *et al*., 2000; Nakagawa *et al*., 2001; Soderling *et al*., 2002; Sun *et al*., 2003).

Here, we have focused our studies on WAVE2, the most widely expressed and leukocyte-dominant WAVE isoform. To directly assess the physiological consequences of a WAVE2 deficiency, we inactivated the WAVE2 gene in the mouse germline to examine its role in murine development and generated WAVE2-deficient cell lines to examine its role in actin-based cell motility.

Results

Gene-targeted inactivation of WAVE2

We used RT–PCR to obtain a WAVE2 cDNA from murine 129sv/ev splenocytes. Human and murine WAVE2 protein sequences share 92.6% identity. We determined that murine WAVE2 RNA, like human WAVE2 RNA, is widely expressed (Suetsugu *et al*., 1999). We mapped the murine WAVE2 genomic locus from a murine 129sv phage library (Stratagene). The WAVE2 gene is encoded by eight exons spanning 20 kb of mouse chromosome 4. To abolish WAVE2 function, we replaced the sequences spanning exons 3–7 with a neomycin-resistance gene (*neo*^{r}) flanked by loxP sites in TC1 embryonic stem (ES) cells (Figure 1A). An IRES–EGFP (intra-ribosomal entry sequence and enhanced GFP) was inserted into intron 2 to allow for the potential assessment of the developmental regulation of the WAVE2 gene upon Cre-mediated excision of the *neo*^{r} marker *in vivo*. We used two independent WAVE2$^{+/neo}$ targeted ES cell lines to generate mice carrying the WAVE2-replacement mutation in the germline (WAVE2$^{+/neo}$ mice) (Figure 1B, Tail southern). To confirm that the targeted replacement of exons 3–7 resulted in loss of WAVE2 RNA and protein expression (Figure 1C), we generated WAVE2$^{neo/neo}$ ES cells by increasing G418 drug selection (data not shown) or by sequential targeting of the wild-type (WT) allele in WAVE2$^{+/-}$ ES cells after Cre-mediated excision of the loxP-flanked *neo*^{r} cassette (Figure 1B, ES targetings, –/neo lane). Immunoblot analyses of WAVE2$^{neo/neo}$, WAVE2$^{-/-}$ ES cells, WAVE2-deficient ES-derived fibroblast-like cells (Figure 1C; data not shown) and WAVE2-deficient mouse embryonic fibroblasts (MEFs; shown below in Figure 5A) all failed to detect WAVE2 protein expression. As we were able to generate WAVE2-deficient ES cell lines, we can conclude that WAVE2 is not required for the survival of ES cells.

WAVE2-deficient embryos have gross morphological defects but normal organogenesis

Mating of WAVE2$^{+/neo}$ male and female mice yielded live WAVE2$^{+/+}$ and WAVE2$^{+/neo}$ pups at the expected Mendelian ratios with no obvious defects in weight or reproductive vigor of the mice. As these breedings failed to yield WAVE2$^{neo/neo}$ progeny (Table I), we performed timed mating and analyzed embryos at various gestational stages to determine when embryonic lethality occurs. Through examination of embryos obtained from embryonic day 7.5 (E7.5) to E17 (confirmed by Southern blot analyses), we determined that WAVE2$^{neo/neo}$ embryos are able to survive through E12–E12.5. Gross examination of dissected WAVE2-deficient embryos shows that they display mild to severe developmental growth retardations (Figure 2A–C). All WAVE2$^{neo/neo}$ embryos showed exterior morphological abnormalities of head and facial structures and posterior limbs and variable abnormalities in body conformation (Figure 2A–C).

Histological analyses of these embryos revealed prominent morphological abnormalities in the appearance of the forebrain and hindbrain ventricles (Figure 2; compare D and F with E and G), reduced ventricle length, and disruption in the cellular organization of caudal somites, the mesodermal tissue which gives rise to muscle, the spinal column and the dermis (Figure 2; compare H and I). As we did not observe an increase in apoptotic cells, the decreased ventricle length and cellular complexity of the caudal somites cannot be attributed to increased cell death (data not shown). In some instances, we also observed hemorrhaging throughout the embryo body (Figure 2C, mut).

Despite developmental delays, there was no apparent neural tube or cardiac abnormalities as observed for a deficiency in N-WASP (Snapper *et al*., 2001). In all the embryos examined, we observed normal organogenesis of the fetal liver and heart and normal extra-embryonic placental tissue when compared with WAVE2$^{+/+}$ and WAVE2$^{+/neo}$ littermates (data not shown). Therefore, the exact cause of embryonic lethality, although undetermined, cannot be attributed to a placental defect. The observed embryonic lethality resulting from WAVE2 deficiency is also not due to *cis* effects from insertion of the *PGK-neo*^{r} cassette on neighboring genes. We generated WAVE2$^{+/-}$ mice by crossing WAVE$^{+/neo}$ mice to Cre-expressing EIIA-Cre/CD1 mice, which delete during the zygotic stage of embryonic development (Lakso *et al*., 1996). Interbreeding of the resulting WAVE2$^{+/-}$ mice did not give rise to viable WAVE2$^{-/-}$ pups (Table I).

Analyses of MEFs isolated from E9.5 and E11 WAVE2$^{neo/neo}$ knockout (KO) embryos indicated a striking reduction in proliferation when compared with WAVE2$^{+/neo}$ (Het) and WAVE2$^{+/+}$ wild-type (WT) MEFs (Figure 3A), whereas WAVE2$^{neo/neo}$ and WAVE2$^{-/-}$ ES cells grew normally (Figure 3B). The proliferation of WAVE2-deficient MEFs was partially restored by ectopic expression of a WAVE2-expressing retrovirus (Figure 3A, RVW2). This partial versus a full restoration of growth may reflect factors including the efficiency of transduction of the WAVE2 retrovirus (~30%) and differential regulation of the ectopic WAVE2 protein expression in the KO MEFs. We conclude that, although WAVE2 is not required for the

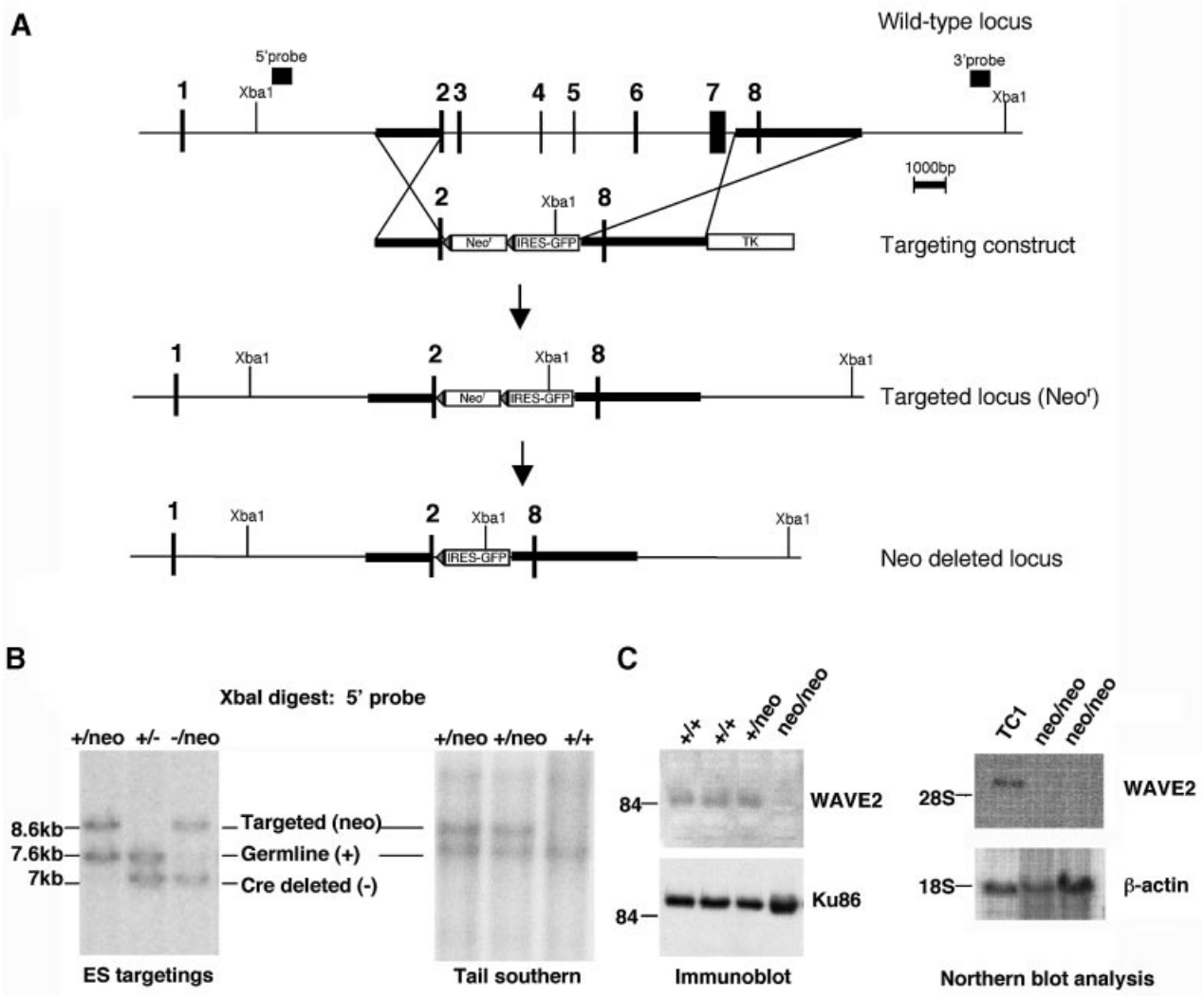

Fig. 1. Murine WAVE2 RNA expression and targeted disruption of WAVE2 in mice and cells. (**A**) Diagram of murine WAVE2 genomic locus and targeting strategy. The physical map of the entire WAVE2 genomic locus containing all eight exons is shown. Exons are indicated by small rectangular boxes. Genomic DNA fragments used to generate the targeting construct are hatched. The neomycin-resistance (Neo^r) and thymidine kinase (TK) genes used for positive and negative selections, the 5′ and 3′ probes, and the *Xba*1 restriction sites used for screening embryonic stem (ES) cell transfectants by Southern blot analyses are labeled. Deletion of the loxP-flanked *neo^r* cassette leaves a single loxP site and the GFP downstream of an intra-ribosomal entry sequence (IRES). (**B**) Generation of WAVE2$^{+/neo}$, WAVE2$^{neo/neo}$ and WAVE2$^{-/neo}$ ES cells and germline mice. Using the 5′ probe noted in the schematic in (A), homologous recombination results in the loss of a single 7.6 kb band and the appearance of a 8.6 kb targeted band or a 7 kb Cre deleted band. Genotypes of germline WAVE2$^{+/neo}$ mice born from mating a WAVE2 chimeric male and a 129sv/ev wild-type female are shown. (**C**) Loss of WAVE2 protein and RNA expression in WAVE2-deficient ES cells. Western blot analyses of protein extracts from wild-type (+/+), WAVE2$^{+/neo}$ (+/neo) and WAVE2$^{neo/neo}$ (neo/neo) ES cells. WAVE2 runs at the 84 kDa molecular weight marker and is absent in WAVE2-deficient ES cells. Equal protein loading was determined using an antibody to Ku86 (Santa Cruz). Northern blot analysis was determined using a WAVE2 cDNA probe. Equal RNA loading was determined with a β-actin control probe.

proliferation and survival of ES cells, it is required for the normal proliferation of MEFs.

We further determined that the slower progression of KO MEFs is not due to an increase in apoptosis, as measured by Annexin V staining of cells (Figure 3C), whereas the percentage of replicating cells in asynchronous MEF populations measured by bromodeoxyuridine (BrdU) incorporation appeared to be significantly reduced (Figure 3D and E). Compared with WT MEFs, 70% fewer KO MEFs were in S phase, indicating that at any given time KO MEFs contained fewer replicating cells (Figure 3D). To track the kinetics of S phase entry of total asynchronous MEF populations, WT and KO MEFs were continuously labeled with BrdU-containing media and sampled for up to 48 h (Figure 3E). KO MEFs consistently displayed markedly fewer cells in S phase than WT MEFs. At 48 h, >89% of WT MEFs incorporated BrdU, compared with <43% of KO MEFs. We conclude that the reduced proliferation of KO MEFs is associated primarily with slower cell cycle progression.

The significant decrease in growth rate of WAVE2 KO MEFs led us to establish fibroblast cell lines by introducing retrovirus that expresses the human papilloma virus E6 and E7 proteins into these MEFs. Transduction of the E6 and E7 proteins into primary cells has been shown to promote long-term culturing of cells through inactivation of p53 and Rb (von Knebel Doeberitz *et al*., 1994; Foster and Galloway, 1996; Furukawa *et al*., 1996; Spitkovsky *et al*., 2002). Independent fibroblast cell lines of each genotype derived from the MEFs (Figure 3) were

Table I. WAVE2 deficiency results in embryonic lethality during mid-gestation

Gestational age[a]	+/+	+/neo	neo/neo	Resorbed	Total
Neonate/birth	45	81	0	nd	126
>E13	17	23	0	10	50
E12–E12.5	2	4	1	2	9
E11.5–E12	11	18	10	3	42
E9.5–E11.5	9	16	11	0	36
E7.5–E8.5	5	14	7	0	26
Gestational age[b]	+/+	+/–	–/–	Resorbed	Total
Neonate/birth	23	51	0	nd	74

Live pups and embryos were genotypes by Southern blot analyses of yolk sac or tissue from embryos.
[a]Offspring from WAVE2$^{+/neo}$ matings;
[b]Offspring from WAVE2$^{+/-}$ matings; nd, not determined.

established. As has been previously reported for other cell types (von Knebel Doeberitz *et al*., 1994; Furukawa *et al*., 1996; Spitkovsky *et al*., 2002), transduction of the E6/E7 retrovirus also changed proliferation capacity of the KO fibroblasts, such that they grew normally, comparable with WT and Het fibroblast lines (data not shown). However, their responses to growth factor stimulation and Rac activation (described below) remain similar to that of primary KO MEFs.

WAVE2-deficient MEFs display defects in actin-cytoskeletal formations

WAVE2 has been implicated in lamellipodium formation downstream of the small GTPase Rac (Miki *et al*., 1998b), which is in turn activated by various growth factors, such as platelet-derived growth factor (PDGF) (Bishop and Hall, 2000). To gain insights into the function of WAVE2 protein in actin-cytoskeletal regulation, primary MEFs generated from WAVE2$^{neo/neo}$ embryos were used to characterize the role of WAVE2 in actin-cytoskeletal organization (Figure 4). WT and WAVE2 KO MEFS were serum starved overnight (in 1% FCS) and then stimulated with PDGF (20 ng/ml) for 10 min (Figure 4A). Quiescent (unstimulated) or PDGF-stimulated cells were stained with TRITC-phalloidin to detect the actin cytoskeleton (red panels) and immunostained with antibody to cortactin to detect membrane ruffles (green panels), represented by circular membrane ruffles (blue arrows) or lamellipodia (yellow arrows) (Figure 4A). Cortactin, a protein implicated in lamellipodium formation downstream of both PDGF and Rac (Weed *et al*., 1998), localizes specifically to membrane ruffles, including circular membrane ruffles and lamellipodia, giving us a sensitive method to differentiate between the different ruffling capabilities of all cells examined in our assay. We observed continuous staining of cortactin and actin along the border of WT MEFs, termed the leading edge, that was predominantly either missing or irregularly dispersed at tips of membrane protrusions in KO MEFs (Figure 4A; compare WT and KO, indicated by yellow arrows).

Quantitative analyses of 100 WT and KO MEFs (counted independently by two investigators blinded to the conditions used) show that circular membrane ruffle formation observed upon PDGF stimulation and lamellipodia formation under both unstimulated and PDGF-stimulated conditions are severely compromised in KO MEFs (Figure 4C). KO MEFs exhibit ~10-fold less circular membrane ruffle formation and 4-fold less lamellipodia formation than WT MEFs (Figure 4C; the average of eight experiments for each condition is shown). We find that the KO MEFs exhibit more accentuated cytoskeletal defects, consistently displaying aberrant cortactin staining compared with WT MEFs (Figure 4C, PDGF; cortactin panels are in green, circular ruffles are indicated by blue arrows and lamellipodia by yellow arrows). Further, we consistently observed that KO MEFs show increased stress fibers (shown in bright field images in movies 3 and 4 of the Supplementary data available at *The EMBO Journal* Online) and low actin staining in the lamellipodia, whereas WT MEFs show more prominent actin staining in the lamellae under both quiescent and PDGF-stimulated conditions. We conclude that WAVE2 is required for proper lamellipodia formation under normal and induced cell growth conditions and for the proper induction of circular membrane ruffles by PDGF. Similar results were obtained using E6/E7 transformed WAVE2 Het and KO fibroblast lines. In contrast, we find that the formation of focal adhesion complexes, examined by colocalization of VASP and actin, were comparable between KO and WT MEFs (data not shown).

We used live video-microscopy to analyze the motile response of WT (movies 1 and 2 in the Supplementary data) and KO (movies 3 and 4) MEFs to PDGF. WT MEFs responded strongly to PDGF, displayed increased motility and produced large circular ruffles and lamellipodia (movie 2); KO MEFs displayed less extensive motility and lamellipodia and almost complete absence of circular ruffles (movie 4). Filopodia formation was qualitatively observed at similar levels in both WT and KO MEFs in both unstimulated and PDGF-induced conditions (movies 1–4) and upon stimulation with bradykinin (movies 5 and 6). Further, we assessed the chemotactic response of KO MEFs to PDGF and found that the migration of KO MEFs was clearly reduced compared with WT MEFs (Figure 4 D). We conclude that WAVE2 is required for the motility and formation of membrane ruffles induced by PDGF in MEFs.

To confirm that the absence of WAVE2 protein is the cause of the observed cytoskeletal defects, we sought to rescue the phenotype by ectopic expression of WAVE2 with a bicistronic retroviral vector containing the WAVE2 cDNA and EGFP. Figure 4B shows KO cells that express the transduced WAVE2 protein (RVWAVE2) stained for cortactin (red panels) and actin (blue panels). KO cells in which WAVE2 expression was restored have normal membrane ruffle morphology and increased percentage of lamellipodia and circular membrane ruffle formation both in the quiescent state (unstimulated) and after PDGF stimulation. We conclude that the WAVE2 deficiency is the direct cause of the cytoskeletal defects observed in WAVE2-deficient fibroblasts.

We examined the levels of WAVE1 (using two different antibodies) and N-WASP in the WAVE2-deficient fibroblasts and did not detect any significant changes in the protein expression patterns of these proteins in lysates lacking WAVE2 (Figure 5A). Therefore, we can conclude that the WAVE2 deficiency does not result in either a

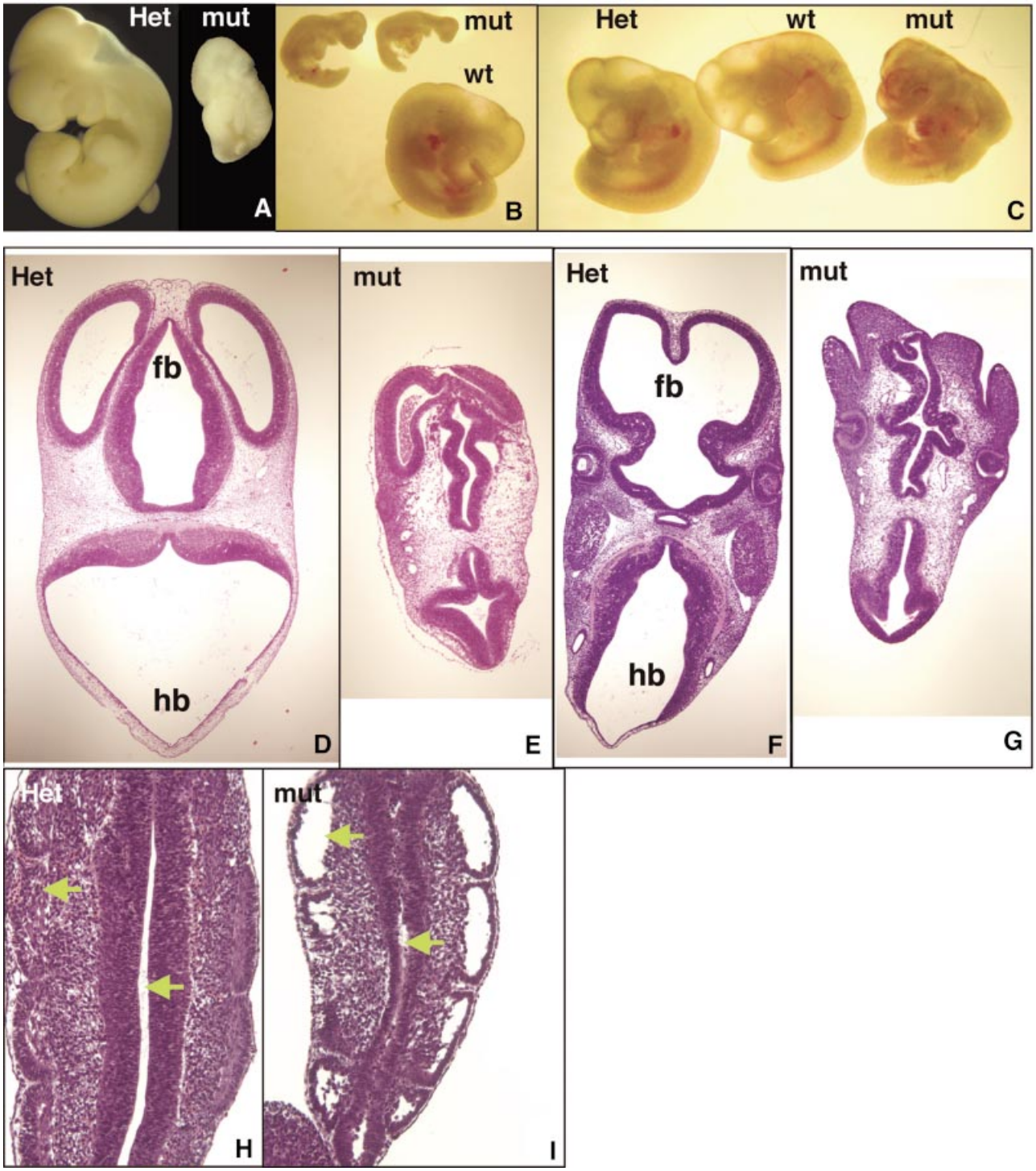

Fig. 2. WAVE2 deficiency results in mild to severe growth retardation and profound morphological defects in embryos. (**A**–**C**) Micrographs of E11–E12 wild-type (wt), WAVE2$^{+/neo}$ (Het) and WAVE2$^{neo/neo}$ (mut) embryos derived from F1 WAVE$^{+/neo}$ matings. Embryo littermates were photographed together at 20× (B and C) or 40× (A) magnification. The micrograph in (A) shows embryos fixed in Bouin's Solution (Sigma); (B) and (C) show micrographs of unfixed embryos. Distinct growth retardations of mut versus wt embryos are apparent in (A) and (B). Branchial arches, limb buds, somites (A, B and C) and blood (B and C) are apparent. In (C), the mut embryo is comparable in size to wt and Het littermates but displays distinct conformational abnormalities: decreased size and malformation of cephalic (head) and caudal extremities and increased hemorrhaging. (**D**–**I**) High-powered hematoxylin-eosin staining of the transverse sections of WAVE2$^{+/neo}$ (Het) and WAVE2$^{neo/neo}$ (mut) embryo littermates. (D, E, F and G) Transverse section of 6–7 μm thickness taken from the cephalic region of WAVE2$^{+/neo}$ (D and F) and WAVE2$^{neo/neo}$ (E and G). The forebrain (fb) is oriented at the top and the hindbrain (hb) at the bottom. More anterior section (D and E) displaying the three ventricles of the forebrain (fb) and later sections (F and G) displaying lens and cheek formation are shown. Significant malformations of ventricles in both the forebrain and hindbrain are apparent. (H and I) Transverse section of WAVE2$^{+/neo}$ (H) and WAVE2$^{neo/neo}$ (I) caudal somites. Arrows point to two of several regions that display unusual detachment of cells.

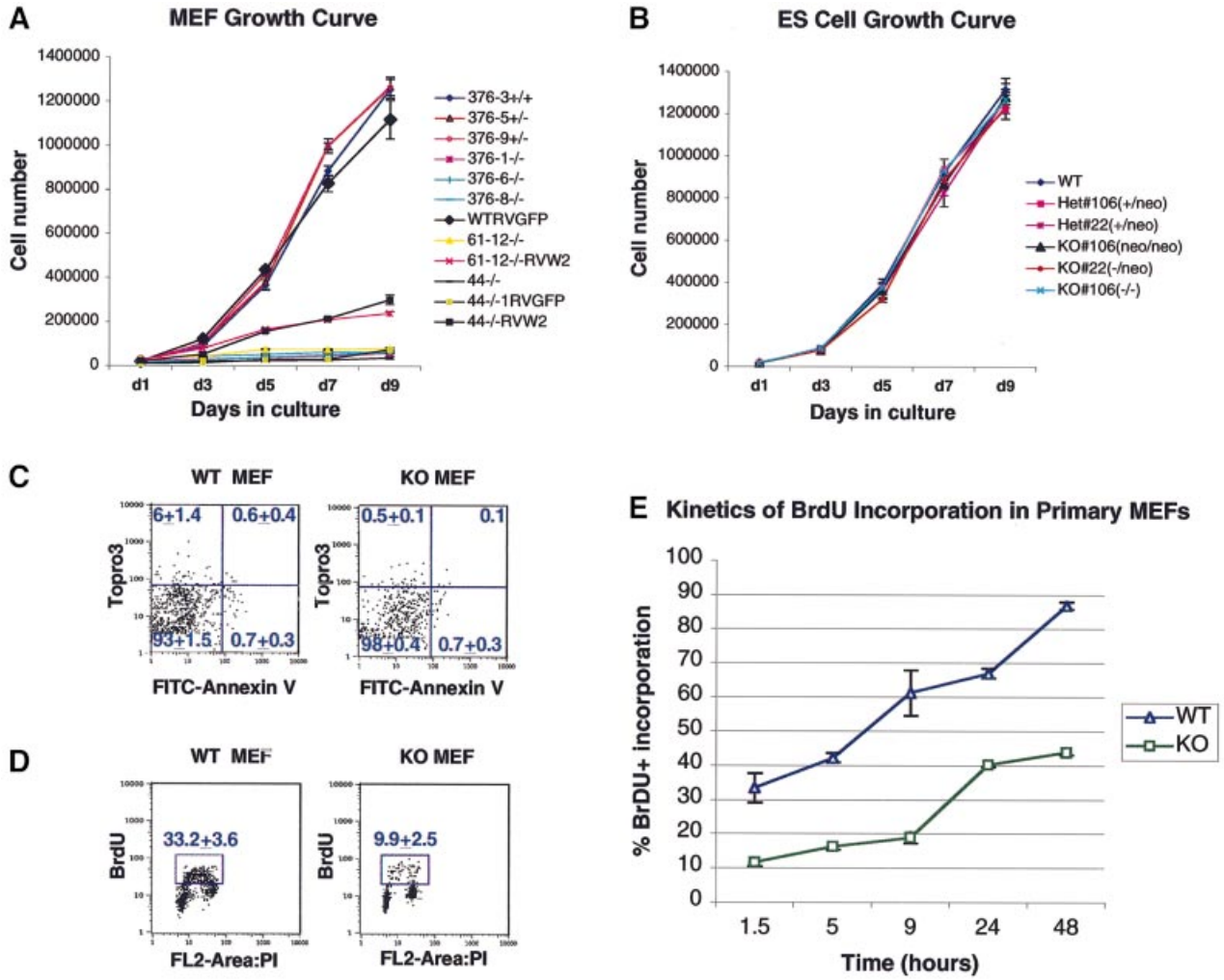

Fig. 3. Growth rate of WAVE2-deficient cell lines. (**A**) Comparison of the growth rate of primary mouse embryonic fibroblasts (MEFs) derived from E11 embryo littermates, one wild-type (376-3+/+), two WAVE2$^{+/neo}$ (376-5+/– and 376-9+/–) and three WAVE2$^{neo/neo}$ MEFs (376-1–/–, 376-6–/– and 376-8–/–), and the growth rates of primary MEFs, untransduced (44–/– and 61-12–/–) or transduced with retrovirus expressing GFP (WTRVGFP and 44–/–RVGFP) or the WAVE2–GFP (61-12–/–RVW2 and 44–/–RVW2). Early passage cells were plated at 2×10^4 per well in a 6-well dish in triplicate fashion. Cells were counted every 2 days up to 9 days in two independent experiments. The average of each experimental point with standard error bars is shown (hatched bars). Additional growth curves of primary MEFs derived from E9.5 embryo littermates gave similar results (data not shown). (**B**) The growth rate of WAVE2-deficient (KO) embryonic stem (ES) cells containing or lacking the loxP-flanked *neo*^{r} cassette are compared with wild-type (WT) and two Het ES cell lines. The genotypes of the ES cell lines are depicted. ES cells, depleted of MEFs, were plated at 2×10^4 cells per well in a 6-well dish and counted in triplicate as described above. The average of each experimental point with standard error bars is shown (hatched bars). (**C**) Flow cytometric analyses of FITC-Annexin V binding versus Topro 3 uptake in WT versus KO MEFs. Upper left, damaged cells (Annexin V$^-$, Topro 3$^+$); lower left, live cells (Annexin V$^-$, Topro 3$^-$); upper right, late apoptotic and dead cells (Annexin V$^+$, Topro 3$^+$); lower right, early apoptotic cells (Annexin V$^+$, Topro 3$^-$). Numbers represent the average of three experiments. (**D**) WAVE2 KO MEFs contain fewer replicating cells. WT and KO MEFs were pulsed for 1.5 h with 20 μM bromodeoxyuridine (BrdU) and analyzed by flow cytometry. The average percentage of labeled cells among total live cells from three experiments is indicated by the box. (**E**) Kinetics of BrdU incorporation of WT versus KO MEFs. MEFs were continuously labeled with 100 μM BrdU for 48 h and analyzed by flow cytometry. The average percentage of BrdU-labeled cells among total live cells from three experiments with standard error bars is plotted at each time point.

compensatory increase or decrease in the stability of WAVE1 or N-WASP protein expression. However, we were unable to specifically determine whether WAVE3 protein expression is affected in the absence of murine-specific WAVE3 antisera. We further performed RT–PCR to examine the level of expression of all three WAVEs in WT versus KO MEFs (Figure 5B). Our results demonstrate that all three WAVEs are expressed in MEFs and confirm that there is no significant change in WAVE1 expression in the absence of WAVE2. WAVE3 expression was barely detectable in WT MEFs, and we did not observe any clear-cut difference in this low-level expression in KO MEFs (Figure 5B).

Rac-induced actin polymerization is abolished in WAVE2-deficient MEFs

Rac signaling to actin *in vitro* has been shown to involve an activatable WAVE complex (Eden *et al*., 2002). To assess the requirement for WAVE2 in actin assembly, we tested WAVE2-deficient lysates generated from MEFs for the ability to activate the Arp2/3 complex using an *in vitro* pyrene-labeled actin polymerization assay (Figure 6). Immunoblot analyses of WAVE2 protein expression in the MEFS used in the studies described below are shown in Figure 5A. WAVE2$^{+/neo}$ lysates responded to both GTPγS-charged Rac1 and GTPγS-charged Cdc42 (Figure 6A). However, in the absence of WAVE2, actin polymerization

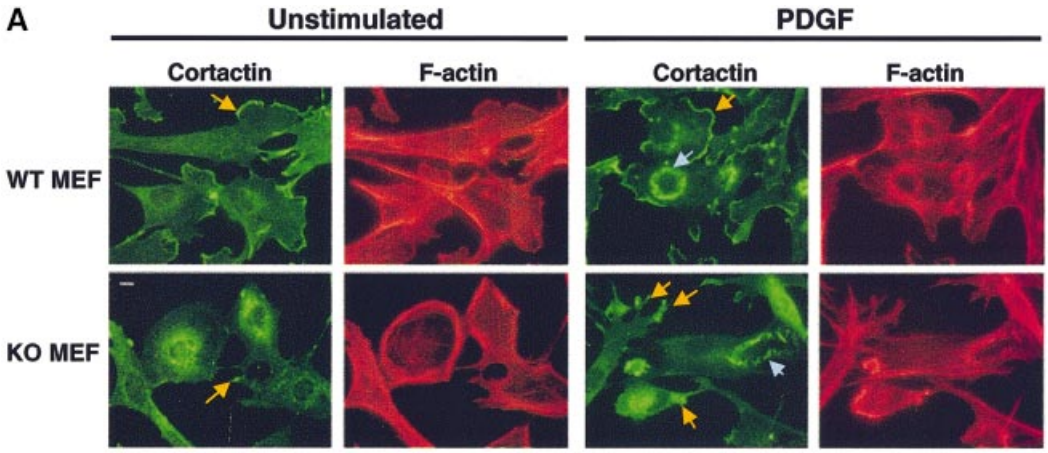

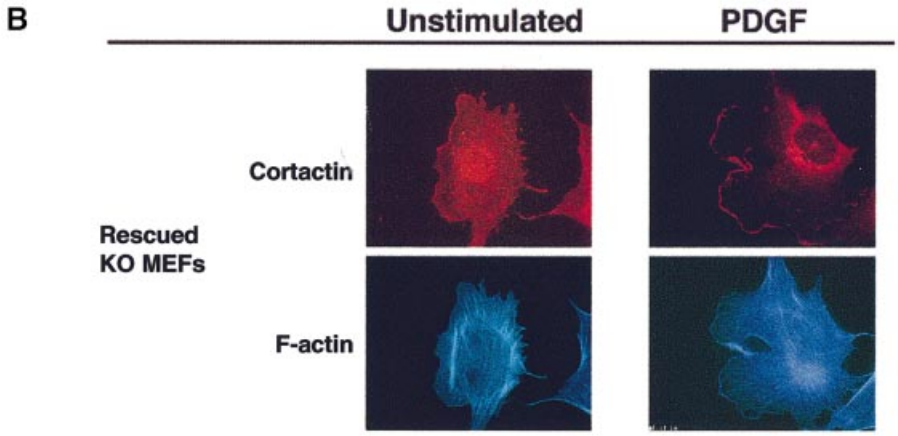

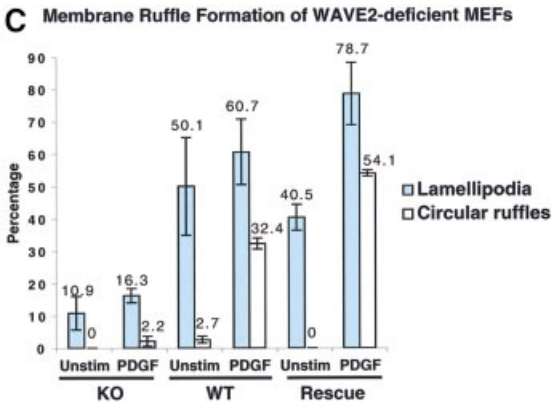

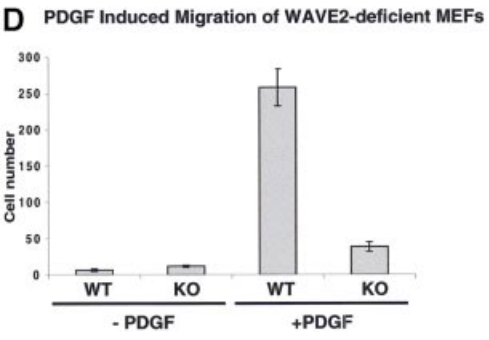

Fig. 4. WAVE2 is essential for lamellipodium and ruffle formation in mouse embryonic fibroblasts (MEFs). (**A**) Sub-confluent serum-starved wild-type (WT) and WAVE2 knockout (KO) MEFs were left unstimulated or stimulated with 20 ng/ml PDGF for 10 min. The leading edge and other areas of lamellipodia and ruffles are more obvious by cortactin staining (green panels) and detection of F-actin cytoskeleton by TRITC-phalloidin (red panels). KO cells show more distinct cytoskeletal defects. Note the absence of leading edge and aberrant lamellipodia formation (yellow arrows point to leading edge of lamellipodia) in unstimulated KO cells compared with WT cells. PDGF induces lamellipodia (yellow arrows), and circular ruffles (blue arrows) in KO MEFs are structurally malformed. Scale bar, 10 μm. (**B**) WAVE2 retroviral expression rescues the defect in lamellipodium formation. WAVE2 KO MEFs transduced with WAVE2 retrovirus (RVWAVE2), left unstimulated or stimulated with 20 ng/ml PDGF for 10 min. Cortactin staining is shown in red and F-actin in blue. Rescued KO MEFs exhibit a normal morphology with well-defined lamellipodium areas. (**C**) Membrane ruffle formation of WT, KO and Rescue (KO MEFs rescued with the WAVE2 retrovirus). One hundred cells of each condition were counted. Membrane ruffles are broken down into two distinct categories: lamellipodia and circular ruffles. Numbers represent an average of more than eight independent experiments performed for WT and KO and more than three experiments for the Rescue conditions. The average of these conditions with standard error bars is shown. (**D**) The chemotactic response of WT and KO primary MEFs to PDGF was examined under conditions containing (+PDGF) or lacking (-PDGF) PDGF at 10 ng/ml. The graph depicts the average of three experiments (42 fields of cells per condition) counted at two magnifications.

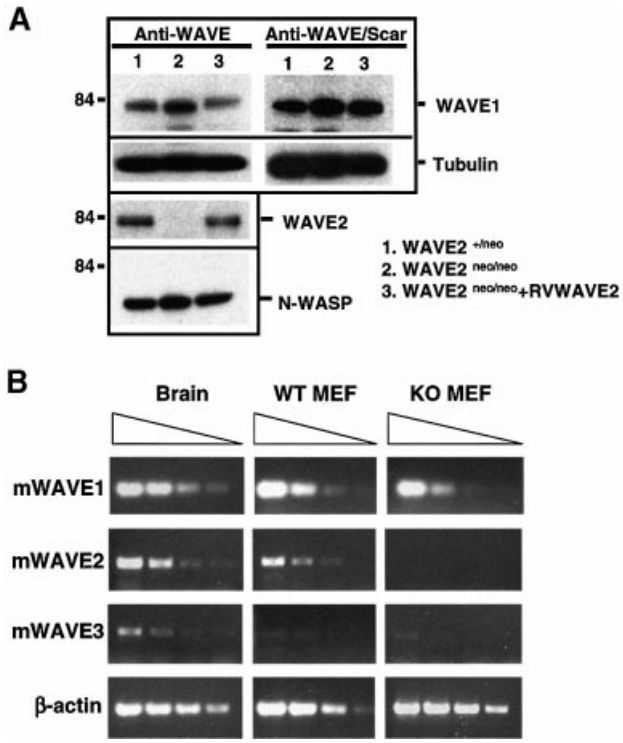

Fig. 5. (**A**) Western blot detection of WAVE1, WAVE2 and N-WASP in wild-type (WT) and knockout (KO) mouse embryonic fibroblasts (MEFs). The genotypes of the MEFs examined are depicted. The 84 kDa standard protein marker is shown. (**B**) RT–PCR analyses of WAVE1, WAVE2 and WAVE3 expression levels in WT and KO MEFs and in brain. β-actin is used as a control. PCRs were performed with 5-fold dilution of cDNAs from left to right.

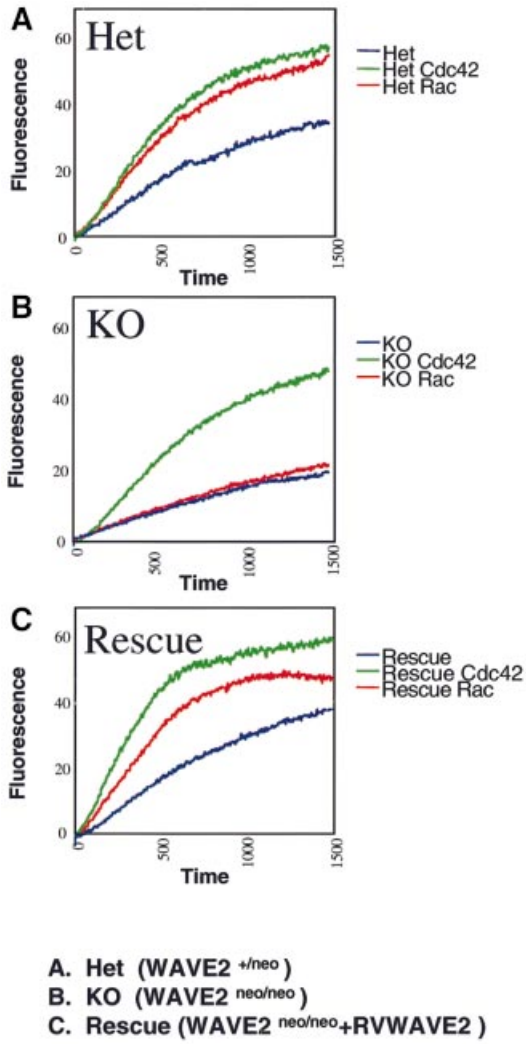

Fig. 6. GST–Cdc42 or GST–Rac induced actin polymerization in WAVE2-deficient cell extracts. Kinetics of actin polymerization in the absence (blue) or presence of GTPγS-charged GST-Rac (green) or GTPγS-charged GST–Cdc42 (red). (**A**) Het (WAVE2$^{+/neo}$); (**B**) KO (WAVE2$^{neo/neo}$); (**C**) Rescue (WAVE2$^{neo/neo}$+RVWAVE2).

mediated by GTPγS-charged Rac1 is completely abolished (Figure 6B), whereas GTPγS-charged Cdc42 activation is comparable between the WAVE2$^{+/neo}$ and WAVE2$^{neo/neo}$ lysates. The results from these studies using activated Cdc42 ensured that the downstream actin assembly components in these lysates were intact and demonstrated that WAVE2 is not essential for Cdc42-mediated actin polymerization.

To ensure that the defect in actin assembly in WAVE2-deficient cells directly correlated with loss of WAVE2 function, we examined the actin assembly of WAVE2$^{neo/neo}$ extracts in which WAVE2 protein expression (using WAVE2 retrovirus RVWAVE2) was reconstituted *in vivo*. This method of reconstitution rescued the ability of WAVE2-deficient extracts to respond to GTPγS-charged Rac1 activation of actin assembly (Figure 6C). Recombinant WAVE proteins, in the absence of protein complexes that attenuate its function, can constitutively stimulate actin polymerization *in vitro* (Machesky *et al*., 1999; Eden *et al*., 2002). Therefore, the lack of actin nucleation in the absence of GTPγS-charged Rac1 or Cdc42 in these lysates also demonstrates that the ectopic expression of WAVE2 cDNA by the retroviral long terminal repeat in WAVE2-deficient cells did not create a pool of uncomplexed and constitutively active WAVE2 protein. Our studies unequivocally demonstrate that WAVE2 is critical for Rac-mediated actin assembly in MEFs.

Discussion

The early requirement of a gene for developmental progression is often marked by histological abnormalities detected at different stages up to the time of death. This is true for murine inactivation of Cdc42, which is embryonic lethal at E3.5 during implantation (Chen *et al*., 2000); Rac1, at ~E8.5 during gastrulation (Sugihara *et al*., 1998); N-WASP, at E11 during early organogenesis (Snapper *et al*., 2001); and WAVE2, by E12.5 during mid-gestation (the present study). Thus, like N-WASP, WAVE2 is not required for signal events downstream of Rho GTPases during early embryonic development, which suggests that alternate signaling pathways involving other WASP-related/associated molecules, or through Rab (Spaargaren and Bos, 1999; Sun *et al*., 2003) or Ras (Miki *et al*., 1999) GTPase pathways, must be utilized to signal gastrulation and cell growth during early embryogenesis.

We have observed several striking morphological anomalies associated with the WAVE2 deficiency: the

disruption of symmetry and size of ventricles of the central nervous system and a decrease in complexity of internal structures that form the caudal somites. A reasonable, but unproven, explanation for the shrunken cerebral ventricles is that there is insufficient cerebrospinal fluid (CSF) pressure to maintain the ventricular distention present in normal embryos. The CSF is regulated by the choroid plexus, a structure formed during mid-gestation at E12.5 (Kaufman and Bard, 1999). We speculate that WAVE2 may play an essential role in the active migration and chemotaxis of particular cell types, such as those involved in the formation of the choroid plexus. Thus, in the absence of WAVE2, reduced cell migration from the neural exis outward towards the cephalic and caudal extremities may account for the extensive morphological anomalies observed.

Since the absence of Rac results in a complete block in axial structure formation (Sugihara *et al*., 1998), the embryonic defects associated with the WAVE2 deficiency may reflect later developmental impairments in Rac signaling. We further speculate that the hemorrhaging observed in some instances may reflect potential functions of WAVE2 in cell adhesion or wound healing. A defect in cell adhesion may explain the decreased complexity or adherence of cells observed in the somites of WAVE2 KO embryos. These findings are also in agreement with functions in cytoplasmic organization and axonal development described for the single SCAR/WAVE mutant allele in *Drosophila* (Zallen *et al*., 2002). One interpretation might be that the requirement for WAVE2 during mid-embryonic development reflects the lack of compensatory WAVE1 and WAVE3 expression. However, as WAVE2 is also expressed in the adult brain, it is more likely that each WAVE isoform in mammalian cells regulates unique functions.

Our studies show that at least two different cell types (ES cells and MEFs) display differential requirements for WAVE2 and demonstrate an essential role for WAVE2 in the growth and actin-based motility of MEFs in response to stimulation by growth factors that promote the activation of early Rac signaling events. We unequivocally demonstrate that cell movement of MEFs and fibroblast lines under normal growth conditions require WAVE2 to form lamellipodia. Further, although WAVE2 is not absolutely essential for the induction of circular ruffles by PDGF, our findings suggest that WAVE2 may attenuate the response to PDGF stimulation.

In response to PDGF, WAVE2 KO cells form circular ruffles that are clearly disorganized, whereas filopodia (microspike) formations mediated by Cdc42 appear qualitatively unaltered. In one report, coinjection of the acidic regions of N-WASP and WASP into macrophage triggered lamellipodia formation in the presence of V12Rac1 (Hufner *et al*., 2002). Therefore, one possible explanation as to why loss of WAVE2 does not abolish circular ruffle formation might be attributed to redundant functions of other WAVE isoforms or N-WASP in the absence of WAVE2. We find that WAVE1 and N-WASP are both clearly detectable in WAVE2-deficient cells (ES cells, MEFs and fibroblasts), with no significant difference in expression levels of these WASP-related proteins.

The current consensus in the actin field is that WASP family members are responsible for spatial extension and duration of membrane protrusions in redundant as well as distinct ways in the same cell (Bailly and Condeelis, 2002; Nozumi *et al*., 2003), Therefore, it is also possible that the generation of a full membrane-ruffling response requires the unique functions of the three WAVE isoforms in conjunction with N-WASP. Thus, as observed in WAVE2 KO MEFs, the loss of one WAVE isoform may facilitate compensatory remodulation of signals that is sufficient for reduced cell motility and altered chemotactic responses. Alternatively, in the absence of WAVE2, as a compensatory measure, cells are able to utilize alternate PDGF responsive pathways (e.g. GTPase Rab5) to induce lamellipodia formation by a novel mechanism independent of, and distinct from, PI3-K, Ras or Rho-family GTPases (Spaargaren and Bos, 1999; Rotsch *et al*., 2001; DesMarais *et al*., 2002). In contrast, the loss of WAVE2 in ES cells does not appear to affect growth, which may reflect the pluripotency and different motility and adhesion characteristics and morphology of ES cells that is absent in fibroblasts.

Our assays using extracts made from WAVE2-deficient MEFs provide direct evidence that WAVE2 is a major regulator of Rac-mediated Arp2/3 activity in MEFs. We note that the detectable expression of the WAVE1 protein by two different antibodies and by RT–PCR is unexpected, since Rac-mediated actin polymerization is abolished in MEFs in the absence of WAVE2. One explanation for this finding is that, *in vivo*, WAVE1 is differentially activatable, requiring additional factors or stimuli to promote actin polymerizaton in different cell types. Alternatively, in the absence of WAVE2, WAVE1 is somehow inactivated by altered protein interactions (Eden *et al*., 2002; Soderling *et al*., 2002). In this regard, since activated Rac is coupled to non-hydrolyzable GTPγS in our assays, the altered interactions cannot be due to altered interactions with the Rac selective GTPase-activating protein WRP.

In preliminary studies, we have also observed that the activation of mitogen-activated protein kinases (MAPKs) is essentially intact in WAVE2-deficient cells. WAVE2 KO MEFs display normal phosphorylation of p38, JNK and IκBα and subtle reductions in ERK (p42 and p44) (C.Yan and F.W.Alt, unpublished data). Thus, the primary cause of embryonic death associated with a deficiency in WAVE2 is more likely due to defects in early cell signaling events that promote cytoskeletal remodeling at the plasma membrane and not by later signaling events to the nucleus. Together, these findings clearly point to additional regulations of WAVE protein functions that require further examination.

Materials and methods

Gene targeting and generation of WAVE2 KO mice

Phage clones containing 20 kb of WAVE2 genomic DNA, with overlapping sequences spanning 7 out of 8 exons, were isolated from a 129λ murine genomic library (Stratagene) using a WAVE2 cDNA probe. A 2 kb *Bam*HI fragment containing exon 2 was blunted and subcloned into a blunted *Sal*I site into pLNTK, 5′ of the loxP-flanked *neo*^{r} cassette. A 3.7 kb *Eco*RI–*Bam*HI fragment containing exon 8 was blunted and cloned into a blunted *Xho*I site, 3′ of the *neo*^{r} cassette behind the GFP downstream of an IRES. The KO vector was targeted into TC1 ES cells using standard methods. Two karyotyped ES cell lines were injected into C57/B6 blastocysts, and germline transmission into the 129sv/ev genetic

background was verified by Southern blot analyses using probes lying outside the homology arms (Figure 1A). To generate mice with *neo*^{r}-deleted mutant alleles, WAVE2$^{+/neo}$ F1 mice were bred with EIIA-Cre/CD1 mice (Lakso *et al*., 1996). The IRES–EGFP, introduced into intron 2, did not show sufficient fluorescence for direct visualization *in vivo*. Detection of murine WAVE1, WAVE2 and WAVE3 (primer pairs derived from cDNA sequences from GenBank) by RT–PCR was performed using Superscript II (Invitrogen).

Preparation and analyses of ES cells and MEFs

ES cells, ES-derived fibroblast-like cells, MEFs and fibroblast lines were prepared using standard protocols (Foster and Galloway, 1996; Chen *et al*., 2000; Snapper *et al*., 2001). For rescue studies, cells were transduced with retrovirus expressing WAVE2–GFP or GFP as described previously (Snapper *et al*., 2001; Klein *et al*., 2003). For proliferation assays, rescue studies were performed on primary MEFs transduced at ~30%, assessed by GFP expression. Stable GFP$^+$ fibroblast lines were established by fluorescence-activated sorting, subcloning and outgrowth of GFP$^+$ cells.

Apoptosis was measured by flow cytometry as described previously (van Engeland *et al*., 1996). For cell cycle analyses, asynchronous primary MEFs were pulse labeled in 20 μM BrdU (Sigma) for 1.5 h or placed in complete Dulbecco's medium containing 15% FCS media and 100 μM BrdU for continuous labeling for up to 48 h. Cells were processed and analyzed by flow cytometry as described previously (Gu *et al*., 1997).

For growth factor stimulation, cells were attached to fibronectin-coated coverslips for 2 days, serum starved (overnight for primary MEFs; 2 days for fibroblast lines) in Iscove's modified Dulbecco's medium containing 1% FCS and stimulated with PDGF (Calbiochem) at 20 ng/ml or bradykinin (Calbiochem) at 100 ng/ml. For time-lapse video-microscopy, PDGF or bradykinin was added through a pipette tip from the outer edge of the field of view, and motility of cells was followed for 10 min using NIH Image 1.62 software at 200× and 400× magnification on a Nikon Eclipse TE200 microscope with a CCD-300-RC Camera (Dage-MTI).

Chemotactic response of primary MEFs (serum starved in 1% FCS media) to PDGF BB (Calbiochem) at 10 ng/ml was examined using a 48-well Boyden chamber (Neuroprobe) through PVP-free polycarbonate filters with 8 μm diameter pores as described previously (Paik *et al*., 2001). After 6 h at 37°C under 5% CO_2, cells that migrated into the lower side of the filters were fixed, stained and counted at 40× and 100× magnifications using a Nikon TMS microscope.

Immunofluorescence

Cells were fixed with 4% formalin solution (Sigma) in PBS at 25°C for 20 min, washed twice with PBS and permeabilized with 0.2% Triton X-100/PBS at 25°C for 5 min. Cells were washed twice with PBS, blocked with 2% BSA/PBS for 10 min and then immunostained with 4F11 (Upstate Biotechnology) anti-cortactin monoclonal antibody at 7 μg/ml for 1 h, washed three times with PBS and counterstained with anti-mouse IgG Alexa 488 conjugated antibody (Molecular Probes) for 1 h. For actin staining, cells were washed with PBS and incubated with 1 μg/ml TRITC-phalloidin (Sigma) or CPITC-phallacin (Molecular Probes) for 20 min at 25°C. Photographs were taken in a fluorescent microscope (Nikon Eclipse E800).

Actin polymerization assay

Cell extracts were prepared as described previously (Chen *et al*., 2000). Pyrene-labeled actin (45% labeling) at 1 μM was added to 1.5 mg/ml extract (final concentration) in 20 mM HEPES pH 7.5, 100 mM KCl, 5 mM $MgCl_2$ and 0.1 mM EDTA. GST–Cdc42 or GST–Rac1 were expressed in SF9 cells, charged with GTPγS and added to a final concentration of 100 nM. The fluorescence was measured for 15–20 min at 21°C using a Carry Eclipse instrument (Varian).

Retroviruses

A retrovirus expressing murine WAVE2 was generated by cloning the coding sequence into a replication-defective retrovirus as previously described (Snapper *et al*., 2001). WAVE2–GFP bicistronic viruses were constructed by cloning GFP (containing an IRES) downstream of WAVE2. Recombinant virus, producing WAVE2–GFP, or GFP control virus were produced upon transient transfection of the packaging cell line 293GPG or 293T as described previously (Klein *et al*., 2003). In brief, supernatant containing retroviral particles was harvested for five consecutive days and concentrated by ultracentrifugation (30 000 *g*) to a final titre of 10^9/ml.

Western blot analysis and antibodies

Protein lysates from ES cells and MEFs were separated by 10.5% denaturing SDS–PAGE and transferred to Immobilon-P PVDF membranes (Millipore) by standard techniques. Total protein was detected on membranes with Ponceau S (Sigma). Antisera to WAVE2 antibody (Santa Cruz), WAVE/Scar (Upstate Biotechnology), anti-WAVE1 (Eden *et al*., 2002) and N-WASP (Rohatgi *et al*., 1999), followed by incubation with HRP-conjugated secondary antibodies (Roche) and detection by ECL (Amersham), were used to examine the expression of these proteins in lysates. Protein loading was detected with anti-tubulin monoclonal antibody DM 1A (Sigma) and anti-Ku86 (Santa Cruz). Western blot analyses of additional MAPK assays (data not shown) were performed using protocols and antibodies as described previously (Chen *et al*., 2000).

Supplementary data

Supplementary data are available at *The EMBO Journal* Online.

Acknowledgements

We thank Mustif Luftig for reagents; Jonathan Walsh for protocols and assistance with retroviral infections; Miguel A.de la Fuente for early discussions and assistance with WAVE2 cDNA probe design; Brianna Monroe for assistance in growth assays; Laurie Davidson, Dan Foy, Nicole Stokes and Caitlin Kennedy for assistance in the generation of WAVE2$^{+/neo}$ mice; Ramiro Massol for technical assistance in microscopy and critical suggestions; and members of the Alt, Geha, Kirschner, Snapper, Kirchhausen and Rosen laboratories for their continued support. This work was supported by grants from the National Institutes of Health (NIH) (to F.W.A, F.S.R, R.G. and S.B.S) and the Howard Hughes Medical Institute (to F.W.A.). C.Y. is supported by an NIH/NRSA postdoctoral training grant; N.M.-Q. by an MEC postdoctoral grant; and S.E. by Human Frontier and European Molecular Biology Organization fellowships.

References

Bailly,M. and Condeelis,J. (2002) Cell motility: insights from the backstage. *Nat. Cell Biol.*, **4**, E292–E294.

Bear,J.E., Rawls,J.F. and Saxe,C.L.,3rd (1998) SCAR, a WASP-related protein, isolated as a suppressor of receptor defects in late *Dictyostelium* development. *J. Cell Biol.*, **142**, 1325–1335.

Benachenhou,N., Massy,I. and Vacher,J. (2002) Characterization and expression analyses of the mouse Wiskott–Aldrich Syndrome Protein (WASP) family member Wave1/Scar. *Gene*, **290**, 131–140.

Bishop,A.L. and Hall,A. (2000) Rho GTPases and their effector proteins. *Biochem. J.*, **348**,241–255.

Chen,F. *et al*. (2000) Cdc42 is required for PIP(2)-induced actin polymerization and early development but not for cell viability. *Curr. Biol.*, **10**, 758–765.

Cory,G.O. and Ridley,A.J. (2002) Cell motility: braking waves. *Nature*, **418**, 732–733.

DesMarais,V., Ichetovkin,I., Condeelis,J. and Hitchcock-Degregori,S.E. (2002) Spatial regulation of actin dynamics: a tropomyosin-free, actin-rich compartment at the leading edge. *J. Cell Sci.*, **115**, 4649–4660.

Eden,S., Rohatgi,R., Podtelejnikov,A.V., Mann,M. and Kirschner,M.W. (2002) Mechanism of regulation of WAVE1-induced actin nucleation by Rac1 and Nck. *Nature*, **418**, 790–793.

Foster,S.A. and Galloway,D.A. (1996) Human papillomavirus type 16 E7 alleviates a proliferation block in early passage human mammary epithelial cells. *Oncogene*, **12**, 1773–1779.

Furukawa,T., Duguid,W.P., Rosenberg,L., Viallet,J., Galloway,D.A. and Tsao,M.S. (1996) Long-term culture and immortalization of epithelial cells from normal adult human pancreatic ducts transfected by the E6/E7 gene of human papilloma virus 16. *Am. J. Pathol.*, **148**, 1763–1770.

Gu,Y. *et al*. (1997) Growth retardation and leaky SCID phenotype of Ku70-deficient mice. *Immunity*, **7**, 653–665.

Hufner,K., Schell,B., Aepfelbacher,M. and Linder,S. (2002) The acidic regions of WASP and N-WASP can synergize with Cdc42hs and Rac1 to induce filopodia and lamellipodia. *FEBS Lett.*, **514**, 168–174.

Kaufman,M.H. and Bard,J.B.L. (1999) In *The Anatomical Basis of Mouse Development*. Academic Press, San Diego, CA, pp. 184–189.

Kim,A.S., Kakalis,L.T., Abdul-Manan,N., Liu,G.A. and Rosen,M.K.

(2000) Autoinhibition and activation mechanisms of the Wiskott–Aldrich syndrome protein. *Nature*, **404**, 151–158.

Klein,C. *et al*. (2003) Gene therapy for Wiskott–Aldrich syndrome: rescue of T-cell signaling and amelioration of colitis upon transplantation of retrovirally transduced hematopoietic stem cells in mice. *Blood*, **101**, 2159–2166.

Lakso,M., Pichel,J.G., Gorman,J.R., Sauer,B., Okamoto,Y., Lee,E., Alt,F.W. and Westphal,H. (1996) Efficient *in vivo* manipulation of mouse genomic sequences at the zygote stage. *Proc. Natl Acad. Sci. USA*, **93**, 5860–5865.

Machesky,L.M. and Insall,R.H. (1998) SCAR1 and the related Wiskott–Aldrich syndrome protein, Wasp, regulate the actin cytoskeleton through the Arp2/3 complex. *Curr. Biol.*, **8**, 1347–1356.

Machesky,L.M., Mullins,R.D., Higgs,H.N., Kaiser,D.A., Blanchoin,L., May,R.C., Hall,M.E. and Pollard,T.D. (1999) SCAR, a Wasp-related protein, activates nucleation of actin filaments by the Arp2/3 complex. *Proc. Natl Acad. Sci. USA*, **96**, 3739–3744.

Miki,H., Sasaki,T., Takai,Y. and Takenawa,T. (1998a) Induction of filopodium formation by a WASP-related actin-depolymerizing protein N-WASP. *Nature*, **391**, 93–96.

Miki,H., Suetsugu,S. and Takenawa,T. (1998b) WAVE, a novel WASP-family protein involved in actin reorganization induced by Rac. *EMBO J.*, **17**, 6932–6941.

Miki,H., Fukuda,M., Nishida,E. and Takenawa,T. (1999) Phosphorylation of WAVE downstream of mitogen-activated protein kinase signaling. *J. Biol. Chem.*, **274**, 27605–27609.

Miki,H., Yamaguchi,H., Suetsugu,S. and Takenawa,T. (2000) IRSp53 is an essential intermediate between Rac and WAVE in the regulation of membrane ruffling. *Nature*, **408**, 732–735.

Nakagawa,H., Miki,H., Ito,M., Ohashi,K., Takenawa,T. and Miyamoto,S. (2001) N-WASP, WAVE and Mena play different roles in the organization of actin cytoskeleton in lamellipodia. *J. Cell Sci.*, **114**, 1555–1565.

Nozumi,M., Nakagawa,H., Miki,H., Takenawa,T. and Miyamoto,S. (2003) Differential localization of WAVE isoforms in filopodia and lamellipodia of the neuronal growth cone. *J. Cell Sci.*, **116**, 239–246.

Paik,J.H., Chae,S., Lee,M.J., Thangada,S. and Hla,T. (2001) Sphingosine 1-phosphate-induced endothelial cell migration requires the expression of EDG-1 and EDG-3 receptors and Rho-dependent activation of $\alpha_v\beta_3$- and β_1-containing integrins. *J. Biol. Chem.*, **276**, 11830–11837.

Pollard,T.D., Blanchoin,L. and Mullins,R.D. (2000) molecular mechanisms controlling actin filament dynamics in nonmuscle cells. *Annu. Rev. Biophys Biomol. Struct.*, **29**, 545–576.

Rohatgi,R., Ma,L., Miki,H., Lopez,M., Kirchhausen,T., Takenawa,T. and Kirschner,M. (1999) The interaction between N-WASP and the Arp2/3 complex links Cdc42-dependent signals to actin assembly. *Cell*, **97**, 221–231.

Rotsch,C., Jacobson,K., Condeelis,J. and Radmacher,M. (2001) EGF-stimulated lamellipod extension in adenocarcinoma cells. *Ultramicroscopy*, **86**, 97–106.

Seastone,D.J., Harris,E., Temesvari,L.A., Bear,J.E., Saxe,C.L. and Cardelli,J. (2001) The WASP-like protein SCAR regulates macropinocytosis, phagocytosis and endosomal membrane flow in *Dictyostelium*. *J. Cell Sci.*, **114**, 2673–2683.

Snapper,S.B. *et al*. (2001) N-WASP deficiency reveals distinct pathways for cell surface projections and microbial actin-based motility. *Nat. Cell Biol.*, **3**, 897–904.

Soderling,S.H., Binns,K.L., Wayman,G.A., Davee,S.M., Ong,S.H., Pawson,T. and Scott,J.D. (2002) The WRP component of the WAVE-1 complex attenuates Rac-mediated signalling. *Nat. Cell Biol.*, **4**, 970–975.

Soderling,S.H., Langeberg,L.K., Soderling,J.A., Davee,S.M., Simerly,R., Raber,J. and Scott,J.D. (2003) Loss of WAVE-1 causes sensorimotor retardation and reduced learning and memory in mice. *Proc. Natl Acad. Sci. USA*, **100**, 1723–1728.

Spaargaren,M. and Bos,J.L. (1999) Rab5 induces Rac-independent lamellipodia formation and cell migration. *Mol. Biol. Cell*, **10**, 3239–3250.

Spitkovsky,D., Hehner,S.P., Hofmann,T.G., Moller,A. and Schmitz,M.L. (2002) The human papillomavirus oncoprotein E7 attenuates NF-κB activation by targeting the IκB kinase complex. *J. Biol. Chem.*, **277**, 25576–25582.

Suetsugu,S., Miki,H. and Takenawa,T. (1999) Identification of two human WAVE/SCAR homologues as general actin regulatory molecules which associate with the Arp2/3 complex. *Biochem. Biophys. Res. Commun.*, **260**, 296–302.

Sugihara,K. *et al*. (1998) Rac1 is required for the formation of three germ layers during gastrulation. *Oncogene*, **17**, 3427–3433.

Sun,P., Yamamoto,H., Suetsugu,S., Miki,H., Takenawa,T. and Endo,T. (2003) Small Gtpase Rah/Rab34 is associated with membrane ruffles and macropinosomes and promotes macropinosome formation. *J. Biol. Chem.*, **278**, 4063–4071.

Takenawa,T. and Miki,H. (2001) WASP and WAVE family proteins: key molecules for rapid rearrangement of cortical actin filaments and cell movement. *J. Cell Sci.*, **114**, 1801–1809.

van Engeland,M., Ramaekers,F.C., Schutte,B. and Reutelingsperger,C.P. (1996) A novel assay to measure loss of plasma membrane asymmetry during apoptosis of adherent cells in culture. *Cytometry*, **24**, 131–139.

von Knebel Doeberitz,M., Rittmuller,C., Aengeneyndt,F., Jansen-Durr,P. and Spitkovsky,D. (1994) Reversible repression of papillomavirus oncogene expression in cervical carcinoma cells: consequences for the phenotype and E6–p53 and E7–pRb interactions. *J. Virol.*, **68**, 2811–2821.

Weed,S.A., Du,Y. and Parsons,J.T. (1998) Translocation of cortactin to the cell periphery is mediated by the small GTPase Rac1. *J. Cell Sci.*, **111**, 2433–2443.

Westphal,R.S., Soderling,S.H., Alto,N.M., Langeberg,L.K. and Scott, J.D. (2000) SCAR/WAVE-1, a Wiskott–Aldrich syndrome protein, assembles an actin-associated multi-kinase scaffold. *EMBO J.*, **19**, 4589–4600.

Zalevsky,J., Lempert,L., Kranitz,H. and Mullins,R.D. (2001) Different WASP family proteins stimulate different Arp2/3 complex-dependent actin-nucleating activities. *Curr. Biol.*, **11**, 1903–1913.

Zallen,J.A., Cohen,Y., Hudson,A.M., Cooley,L., Wieschaus,E. and Schejter,E.D. (2002) SCAR is a primary regulator of Arp2/3-dependent morphological events in *Drosophila*. *J. Cell Biol.*, **156**, 689–701.

Received January 23, 2003; revised April 4, 2003; accepted May 21, 2003